

Coconut Shell as an Alternative Fuel for Hydrotalcite Catalyst Synthesis via the Combustion Method for Biodiesel Production from Waste Cooking Oil

Mohamed Afiq Mohmed Moffit^{a,b*}, Fatihah Suja^a, Irfana Kabir Ahmad^a & Mohd Razealy Anuar^b

^a*Civil Engineering Department, Faculty of Engineering and Built Environment,
Universiti Kebangsaan Malaysia, 43600 Bangi Selangor*

^b*UniKL Malaysian Institute of Chemical and Bioengineering Technology, 78000 Alor Gajah Melaka*

*Corresponding author: afiqmoffit@gmail.com

Received 22 March 2024, Received in revised form 24 July 2024

Accepted 24 August 2024, Available online 30 January 2025

ABSTRACT

Using saccharose (sugar) as fuel to synthesise hydrotalcite via the combustion method to produce biodiesel could potentially have social and economic benefits in the field of renewable energy. However, it could spark a debate on food vs fuel since a higher demand for saccharose in the energy sector while ensuring adequate supply for the food sector could increase the price of saccharose. Therefore, this study proposes utilising a new alternative material from agricultural waste, coconut shell, to synthesise the hydrotalcite catalyst and use it to produce biodiesel from waste cooking oil. This study found that the hydrotalcite synthesised using coconut shell as fuel and calcined at 650 °C (HT-CS 650) yielded 93.25% biodiesel compared to the 74.14% biodiesel yield when synthesising hydrotalcite using saccharose. The XRD showed that the synthesised hydrotalcite retained its layered double hydroxide structure up to 650 °C calcination temperature. The BET analysis showed that the HT-CS 650 has the highest surface area of 115.558 m²/g compared to the 28.326 m²/g surface area of the reference hydrotalcite (HT-SS 650). The HT-CS 650 can be reused for up to three cycles with a minimum biodiesel yield reduction of 9.09%. This study has demonstrated that agricultural waste is a more suitable fuel for synthesising hydrotalcite in the combustion method and using it to improve the transesterification reaction for biodiesel production.

Keywords: Hydrotalcite; biodiesel; transesterification; coconutshell; combustionmethod

INTRODUCTION

Biodiesel, also known as Fatty Acid Methyl Ester, is one of the renewable energies that can be produced from unlimited sources like used or new vegetable oil and animal fat. Biodiesel has many advantages over petroleum diesel due to its renewable, non-toxic, biodegradable and eco-friendly properties (Che Hamzah et al. 2020; Marwan et al. 2015; Rahul et al. 2011). However, biodiesel production is still at a low level of 534 thousand barrels per day compared to distillate diesel, where the global daily refined diesel production in 2017 was 26,471 thousand barrels (Dudley 2018; Zervos 2018). Therefore, rigorous research, development and improvement of biodiesel are crucial to make it a primary complement to petroleum diesel, which

is the primary global energy source.

Edible and non-edible vegetable oils can be used as raw materials in biodiesel production. However, there are criticisms of using these oils in biodiesel production, such as concerns regarding the food versus fuel agenda, food inflation and deforestation (Naylor & Higgins 2018; Ziegler 2013). One alternative to overcome the problem concerning the raw materials for biodiesel production is using used oil, such as the abundantly and readily available waste cooking oil. The community benefits from using used oil in biodiesel production since there is no competition between used oil and food crops, and the food supply will not be affected. Additionally, humans do not consume waste cooking oils, and the food industry often discards them down the drain (Ka et al. 2013; Kabir et al. 2014).

Commercial processes to produce biodiesel use homogeneous acids or base catalysts such as potassium hydroxide, sodium hydroxide and sulfuric acid (Che Hamzah et al. 2020; Huaping et al. 2006; Nayab et al. 2022; Reyero et al. 2013). However, the main disadvantage of using homogeneous acids or base catalysts is the difficulty in product separation and the generation of large amounts of waste during the washing and purification of biodiesel (Gao & Goldfarb 2019; Huaping et al. 2006; Nayab et al. 2022; Reyero et al. 2013). Because of these issues, researchers have explored using heterogeneous catalysts such as BaCeO_3 , CaO , SnSO_4 , SiO_2 , MgO , hydrotalcite and other materials that allow easy catalyst separation through centrifugation (Borges & Diaz 2012; Che Hamzah et al. 2020; Gao & Goldfarb 2019; Huaping et al. 2006; Nayab et al. 2022).

Hydrotalcite (HT) is a Layered Double Hydroxide (LDH) anionic build-up of brucite-like layers (Dávila et al. 2008) with a general chemical formula of $\text{Mg}_6\text{Al}_2\text{CO}_3(\text{OH})_{16}\cdot 4\text{H}_2\text{O}$. HT is a known catalyst used for various applications in the field of science, such as Cannizzaro reaction, fructose isomerisation, photocatalytic degradation of chlorophenol, transesterification and esterification (Bhojaraj et al. 2019; Lee et al. 2021; Ramos-Ramirez et al. 2018; Yabushita et al. 2019). Environmental researchers are showing increasing interest in HT because its synthetic materials consist of magnesium and aluminium, which are non-toxic and abundantly available elements (Coelho et al. 2017). HT has a good transesterification reaction of palm oil to biodiesel with a relatively high recovery percentage ranging from 76.5% (Helwani et al. 2013) to 84% (Gao & Goldfarb, 2019) when using the stirring method. It is robust and does not cause leaching problems in transesterification reactions (Helwani et al. 2013). The recommended water content in oil for the transesterification reaction is less than 0.5% by weight; HT can withstand water presence of up to 1% by weight without affecting the biodiesel yield (Atadashi et al. 2012). In addition, the HT catalyst can be reused in up to three cycles in subsequent transesterification processes (Anuar & Abdullah, 2016; Coelho et al. 2017).

Among the methods for preparing HT are coprecipitation, sol-gel and combustion (Dávila et al. 2008). This study adopted the combustion method because of its simple and time-saving two-step process consisting of precipitation and calcination. The advantages of the combustion method are high purity and homogeneous catalyst (Lazarova et al. 2019). One of the latest developments for increasing the catalytic activity of LDH catalysts is introducing and regulating the type of fuel used during synthesis through the combustion method. Adding organic fuel as a template increases the specific surface area of the HT catalyst to as high as $152 \text{ m}^2/\text{g}$ compared to

the $36.9 \text{ m}^2/\text{g}$ surface area of the reference HT catalyst (Sobhana et al. 2016), thus increasing the biodiesel yield. Previous studies that used organic templates, such as saccharose, corn starch (Coelho et al. 2017), cellulose (Sobhana et al. 2016), rice starch (Ramimoghdam et al. 2015), pollen grains (Hall et al. 2003) and cyclodextrin (Ciobanu et al. 2013), have achieved positive results with the pore size of the LDH structure. Organic templates are also cheap, economical, environmentally friendly and renewable (Ramimoghdam et al. 2015).

In Malaysia, coconut is the fourth most important crop after palm oil, rubber and rice. Malaysia produced 517,518 metric tons of coconuts in 2017 (FAO 2017; Salmah et al. 2013). Each kilogram of coconut can produce 0.152 kg of coconut shell (Bello et al. 2016). Malaysia generated a large amount of agricultural waste in 2018, of which approximately 0.77 million tons were coconut shells. For a long time, the high volume of coconut shells was deemed to have little economic value and was underutilized, thus resulting in environmental issues (Li et al. 2008). The ample availability and low cost of coconut shells motivated researchers to use them in various applications, including in bio composite materials, concrete mixes, asphalt mixes and activated charcoal (Ismail & Isa 2017; Al-Oqla et al. 2023; Herring & Thuo 2022; Higai et al. 2021). In addition, coconut shell contains 19.8% cellulose, 68.7% holocellulose and 30.1% lignin (Daud & Ali 2004), giving it a high calorific value of 4968 kcal/kg (Bello et al. 2016). Since the fuel source utilized in the catalyst synthesis could affect the yield of biodiesel production, as demonstrated by previous works (Ciobanu et al. 2013; Coelho et al. 2017; Hall et al. 2003; Ramimoghdam et al. 2015), it is feasible to use waste material as a fuel source to synthesize hydrotalcite catalysts. This research chose coconut shell as a fuel for HT synthesis because it has a higher calorific value than saccharose and, therefore, can intensify the combustion process and provide the C and H compounds during the HT synthesis. In addition, this study advocates converting coconut shells, a widely available agricultural organic waste in Malaysia, into useful energy. This study produced the HT catalyst for biodiesel production from waste cooking oil (WCO) through transesterification by synthesizing the HT using coconut shell and saccharose as a fuel source template through combustion. It also investigated two parameters of the produced biodiesel: the effect of calcination temperature and type of fuel (coconut shell and saccharose) and the characteristics of the synthesized HT.

The current method for synthesising hydrotalcite via combustion method uses sugar or saccharose as a fuel to construct the layered structure to achieve higher biodiesel yield. Previous researchers have successfully produced hydrotalcite that increased biodiesel yield using this

method (Anuar & Abdullah 2016; Coelho et al. 2017). However, there is a disadvantage in using sugar or saccharose in the combustion method since sugar is a food product, and its use for biodiesel production could have a social impact on society, such as the issue concerning food vs fuel. Using sugar to produce catalysts for generating energy could increase the price of sugar due to the higher demand for sugar. Therefore, this study proposes a novel initiative of using waste products as a sugar substitute to synthesise the catalysts used in biodiesel production. The novelty in this study is substituting saccharose with agricultural waste to produce hydrotalcite via the combustion method.

MATERIALS AND METHODS

MATERIALS AND REAGENTS

The waste coconut shells used in this study were sourced from local grocery stores in Seremban, Negeri Sembilan. The coconut shell was grounded using a pestle and mortar and filtered with a 25 mm mesh. The synthesis of the HT catalyst used the coconut shell powder and saccharose (Sigma Aldrich), magnesium nitrate hexahydrate (HmBG Chemicals), aluminium nitrate nonahydrate (HmBG Chemicals) and sodium carbonate (Merck). The waste cooking oil (WCO) was collected from households and filtered using cloth filters to remove particles and impurities. The materials used in the biodiesel production were WCO, methanol (R&M Chemicals) and the synthesized hydrotalcite. For gas chromatography analysis, n-hexane (Merck) was used as solvent and methyl heptadecanoate (Sigma Aldrich) was used as an internal standard.

SYNTHESIS OF THE HYDROTALCITE

The synthesis of the hydrotalcite catalyst employed the method adapted from Dávila et al. (2008) and Anuar & Abdullah (2016) using an Mg: Al ratio of three. Pre-calculated amounts of magnesium nitrate hexahydrate (6.72 g) and aluminium nitrate nonahydrate (3.28 g) were placed in two different beakers containing 80 ml of deionized water. Both solutions were heated to 80 °C and stirred until all solids dissolved. The two solutions were gently mixed after five minutes, and Na₂CO₃ 20% by weight and fuel 10% by weight of the total weight of metal nitrate were added to the mixture. The mixture was thoroughly stirred and maintained at 80°C until all water had evaporated. The resulting paste was calcined in a furnace at a calcination temperature of 650°C for five minutes residence time. The experiment was repeated for both fuels (saccharose and coconut shell powder). The resulting Mg-Al-O catalyst was ground into powder and then recrystallized by soaking it in a 0.05 M Na₂CO₃ solution for five minutes, filtered and washed with deionized water two times, followed by five hours of drying in an oven. The resulting dry catalyst was stored in an air-tight container. The HT synthesized using saccharose as fuel was designated HT-SS, while the HT synthesized using ground coconut shell was HT-CS. Table 1 presents the catalyst designation and their respective fuel type and calcination temperatures, and Figure 1 shows the flowchart of the hydrotalcite synthesis. Since this study proposed using coconut shells as a new alternative, the effect of fuel is a critical parameter in determining whether fuel affected the catalytic activity of the transesterification reaction. The varying calcination temperatures were also key parameters since they affected the formation of the HT structure.

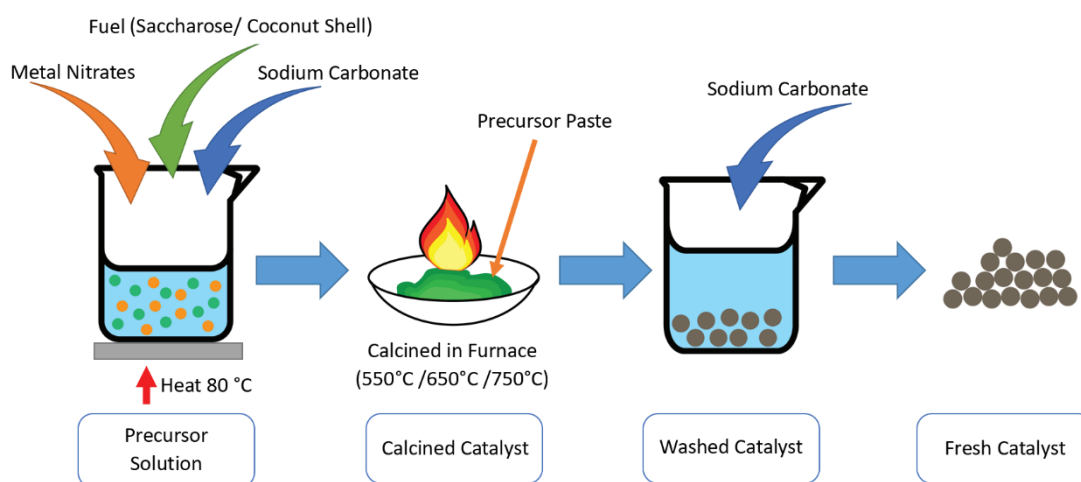


FIGURE 1. Flowchart of Hydrotalcite Synthesis

TABLE 1. Catalyst designation, fuel types and calcination temperatures

Catalyst Designation	Fuel Type	Calcination Temperature (°C)
HT-SS 650	Saccharose	650
HT-CS 550	Coconut Shell	550
HT-CS 650	Coconut Shell	650
HT-CS 750	Coconut Shell	750
HT-CS 850	Coconut Shell	850

BIODIESEL (FAME) PRODUCTION

The transesterification reaction between WCO and methanol was adapted from Anuar & Abdullah (2016), where the reaction was carried out in a double-necked glass reactor immersed in a water bath. The flask was equipped with a condenser and a thermometer. In a typical transesterification reaction, the oil was initially heated for five minutes. Each gram of oil requires 0.08 g of catalyst, which was placed in the reactor at a ratio of 15:1 methanol to oil molar. The reactor was immersed up to its neck to ensure the reaction temperature remained at 65°C during the five hours of the transesterification reaction. The average molecular weight of residual cooking oil was calculated using the formula $M = 56.1 \times 1000 \times 3 / (SV - AV)$, where SV is the saponification value (m_{KOH} / m_{oil} , mg/g), and AV is the acid value (m_{KOH} / m_{oil} , mg/g) (Huaping et al. 2006). After the reaction had completed, the product was centrifuged at 3500 rpm for 30 minutes to separate the top layer, middle layer and bottom layer, which is the biodiesel (FAME), glycerol (by-product), and catalyst, respectively, and the biodiesel layer was analyzed. HT catalyst reusability investigation focused on the most active HT catalysts. After the centrifugation, the bottom layer

(catalyst) was recovered and washed with n-hexane. The recovered HT catalyst was calcined again at 300°C for three hours; the new reactant was used in a new cycle of transesterification reaction under the same conditions. The experimental runs were repeated for three cycles. Figure 2 shows the experimental setup for the biodiesel production.

CHARACTERIZATION OF THE HYDROTALCITE

The crystallinity of the synthesized catalysts was analyzed using X-ray diffraction (X'pert Pro) under 40 kV, 30 mA monochromatic $CuK\alpha$ ($\lambda = 0.15406$ nm) over a 2θ range from 10° to 80°. Analysis of the surface area of the catalyst used the Micromeritics ASAP 2020 surface analyzer, and the functional group of the synthesized catalysts were analyzed using the Nicolet iS10 Fourier Transform Infrared Spectrometer (Thermo Fischer Scientific). The thermal degradation of the freshly prepared catalyst was analyzed using the Mettler Toledo TGA/DSC 1 STAR° System. The analysis for a typical run used approximately 15 mg of catalyst in an N_2 atmosphere (20 cm^3/min). The operating temperature of the analysis was 30°C to 800°C and a ramp temperature of 10 °C/min.

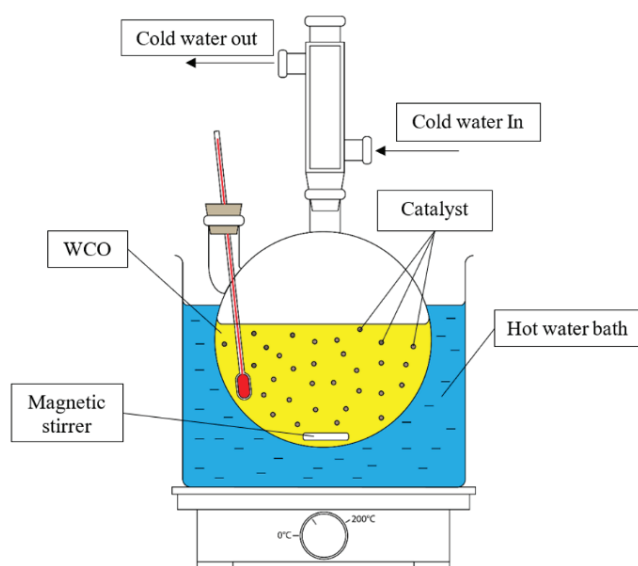


FIGURE 2. Experimental Setup for Biodiesel Production

QUANTIFICATION OF THE BIODIESEL (FAME)

The biodiesel (FAME) obtained via the transesterification was analyzed using a gas chromatograph (Perkin Elmer AutoSystem XL) equipped with an FID and a silica capillary column with a dimension of $30\text{m} \times 0.25\text{ mm} \times 2.5\mu\text{m}$ (Chrompack Search CP-Sil 8CB) and using nitrogen gas as the carrier gas. The method adapted from EN-14103 required weighing approximately 250 mg of the sample in a 10 ml bottle, adding 5 ml of methyl heptadecanoate solution 10 mg/ml into the vial and shaking the mixture vigorously. One μl of the diluted sample was injected into the gas chromatograph, where the ramp rate was $5\text{ }^\circ\text{C}/\text{min}$ to $240\text{ }^\circ\text{C}$. The injector temperature and detector temperature were $250\text{ }^\circ\text{C}$. Analysis of the FAME also used the FTIR Spectrometer (Perkin Elmer Spectrum RX I) for

identification and confirmation by functional group samples.

CALORIMETRIC TEST OF THE FUEL

The study conducted a bomb calorimetric test to determine the calorific value of the fuel (coconut shell and saccharose) employing the Calorimeter P6310 equipped with a Beckmann thermometer. The briquette was produced from one gram of fuel at a pressure of 28 MPa and placed in a crucible. The ignition wire was a stainless-steel wire with a 0.1 mm diameter and a length of 100 mm. The bomb was compressed with $450\text{ lb}/\text{in}^2$ of oxygen and then immersed in 2000 g of water. The fuse wire was ignited when the initial water temperature was constant, and the water temperature was recorded each minute for 20 minutes. Figure 3 presents the experimental flowchart.

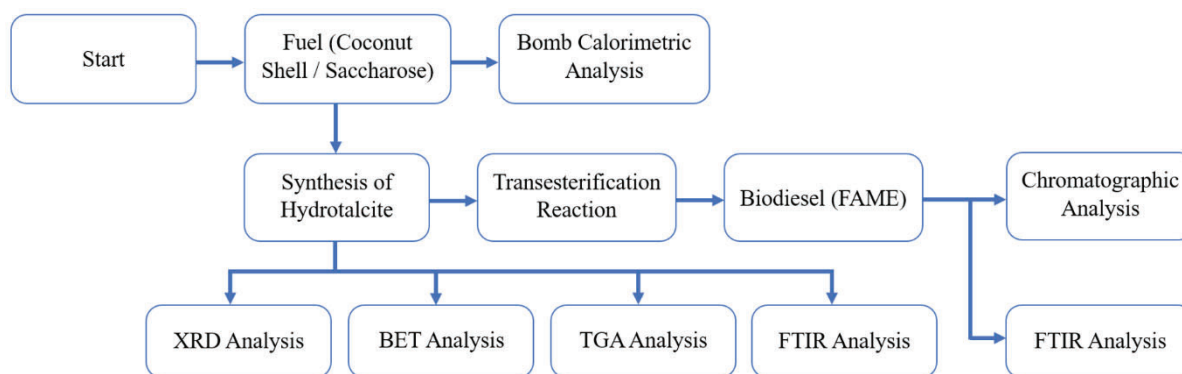


FIGURE 3. The Experimental Procedure.

RESULTS AND DISCUSSION

CHARACTERIZATION OF THE HYDROTALCITE CATALYST

XRD ANALYSIS OF THE HYDROTALCITE CATALYST

The structure and crystallinity of the HT catalyst were confirmed via X-ray diffraction analysis. Figure 4 shows the XRD pattern of recrystallized HT using saccharose and coconut shell as fuel calcined at $550\text{ }^\circ\text{C} - 850\text{ }^\circ\text{C}$. The (1) mark indicates a successful formation of the HT structure, which comprises diffraction peaks at 11.7° , 23.5° , 35.5° , 39.2° , 48.0° , 61.5° and 63.3° per Anuar & Abdullah (2016) and Shekoohi et al. (2017). The HT-SS 650, HT-CS 550 and HT-CS 650 in Figure 4 show the successful synthesis of the HT structure formation as diffraction peaks 11.7° ,

23.5° , 35.5° , 39.2° , 48.0° , 61.5° and 63.3° appeared in the XRD analysis. As reported by previous researchers, the diffraction peaks at 11° and 23° indicated a layered structure (Anuar & Abdullah, 2016; Reyero et al. 2013). These diffraction peaks were present in HT-SS 650, HT-CS 550 and HT-CS 650, thus confirming the formation of layered structure in the samples. However, the absence of 11° and 23° peaks in HT-CS 750 and HT-CS 850 confirms the unsuccessful formation of an HT layered structure. In addition, the x-ray diffractograms for the HT-CS calcined at $550\text{ }^\circ\text{C}$, $650\text{ }^\circ\text{C}$ and $750\text{ }^\circ\text{C}$ show that the intensity of the layered structure decreased with calcination temperature. Treating the HT catalysts at excessively high temperatures caused the layered structure to collapse (Anuar & Abdullah, 2016; Anuar et al. 2013). The high vibration effect due to the excessive exposure to high temperatures (more than $650\text{ }^\circ\text{C}$) resulted in the formation of additional phases. Previous studies reported the diffraction peaks 18.5° and 20.5° , marked (2), as bayerite, or $\text{Al}(\text{OH})_3$ (Fraile et al.

2009). Figure 1 shows that the bayerite compound is present in HT-CS 750 °C, where the diffraction peaks at 18.91° and 20.43°. The low-intensity diffraction peaks at 32.9°, 50.1°, 57.5° and 60.5° and a high diffraction peak at 34.5°, marked as (3), in HT-CS 750 were assigned to Mg(OH)₂ (Selvam et al. 2011). The peaks identified in HT-CS 750 indicate that, at a calcination temperature of 750 °C, the HT thermally decomposed into individual compounds, namely Mg(OH) and Al(OH). On the other hand, the periclase-like structures or MgO peaks at 36.9°, 43.2° and 62.5°, marked (4), were present in the synthesized catalysts (Anuar & Abdullah, 2016, Fraile et al. 2009, Selvam et al. 2011). The most significant periclase-like structure in HT-CS 650, HT-CS 750 and HT-CS 850 is the sharp diffraction peak at 43.2°. The remaining peaks (38.3° and 74.5°) were attributed to Al₂O₃ (Suriyanarayanan et al.

2009). Therefore, it is possible to conclude that calcination at excessively high temperatures facilitated the formation of impurities, decomposition into individual compounds and diminishing memory effect of the HT.

BET ANALYSIS OF THE HYDROTALCITE CATALYST

Table 2 presents the surface characteristics of the synthesized HT. It shows that using coconut shells as fuel in HT synthesis increased its surface area and porosity. HT-SS650 had an initial surface area of 28.326 m²/g and porosity of 0.085 cm³/gm; however, synthesizing HT-SS650 using coconut shells increased its surface area to 115.558 m²/g and porosity to 0.1984 cm³/g, as shown by HT-CS 650.

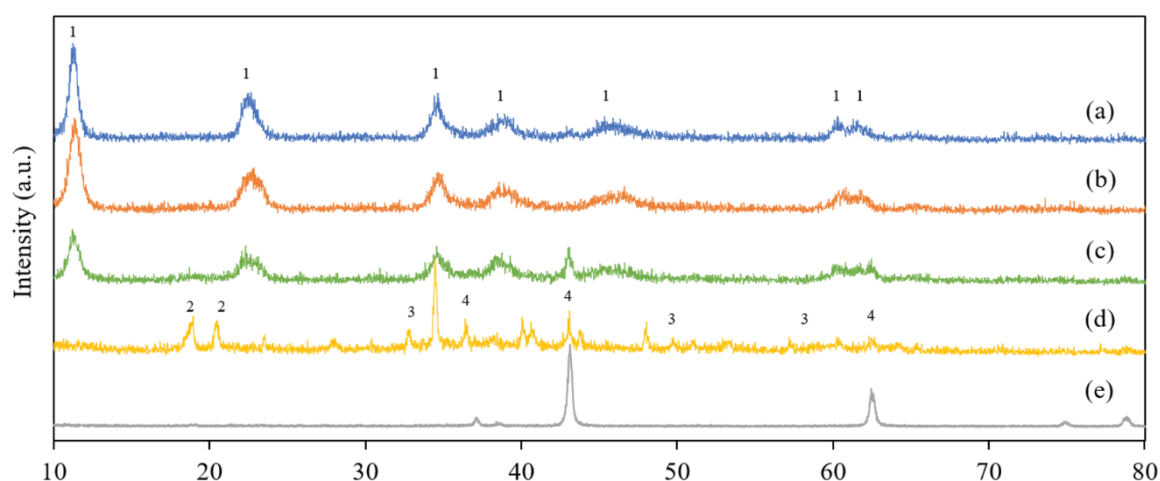


FIGURE 4. XRD patterns of (a) HT-SS 650, (b) HT-CS 550, (c) HT-CS 650, (d) HT-CS 750, (e) HT-CS 850, and (1) HT peaks.

TABLE 2. Surface characteristics of the HT catalysts

Sample	Surface Area (m ² /g)	Pore Volume (cm ³ /g)
HT-SS 650	28.326	0.085
HT-CS 550	79.595	0.263
HT-CS 650	115.558	0.198
HT-CS 750	56.837	0.138
HT-CS 850	28.320	0.303

The increase in surface area and porosity is similar to the findings by Sobhana et al. (2016), where the surface area and porosity of HT increased from 36.900 m²/g and 0.083 cm³/g to 152.000 m²/g and 0.792 cm³/g when using cellulose as fuel in HT synthesis. The high explosion resulted in the formation of the surface area and pore framework by the coconut shells on the HT. The calorific value of the coconut shells was higher than that of saccharose, as shown by the calorific value of saccharose and coconut shell presented in Table 3.

TABLE 3. The calorific value of the tested fuel

Fuel Type	Calorific value (cal/g)
Saccharose	3786.430
Coconut Shell	4233.095

The result of the bomb calorimetric test to determine the calorific value of saccharose and ground coconut shells presented in Table 3 shows that one gram of ground coconut shell has 446.665 higher calories than one gram of saccharose. The higher calorific value is due to

hemicellulose, cellulose and lignin contains a variety of saccharide and hydroxycinnamic alcohol (Kim et al. 2016; Yang et al. 2007). During the catalyst synthesis, the fuel acted as a source of C and H that intensified the combustion during calcination (Dávila et al. 2008). During the calcination, the fuel combusted and produced the CO₂ and H₂O (Helwani et al. 2013) absorbed by the metal oxide periclase-like structure. The CO₂ served as a probe molecule on the surface of the oxide compounds, where monodentate, bidentate and bridged were absorbed, thus facilitating the formation of the carbonate on the surface, which is known as a layered structure (Dávila et al. 2008). The high calorific value provided by ground coconut shells resulted in a higher CO₂ and H₂O production than saccharose, thus facilitating the absorption of the metal oxide and formation of the layered structure and increasing the surface area (Anuar & Abdullah, 2016). The coconut shell fuel produced an 87.232 m²/g larger surface area on the catalyst than the saccharose fuel at the same calcination temperature (650 °C). The large surface area provided a more active site and thus a higher likelihood for a catalytic reaction to occur, thereby increasing the yield of FAME since most reactions prefer a catalyst with a high surface area, as proven by the BET analysis of the HTs calcined at 650 °C and demonstrated by previous research (Anuar & Abdullah, 2016; Gao & Goldfarb, 2019; Helwani et al. 2013, Rahul et al. 2011).

Table 2 shows that increasing the calcination temperature from 550 °C to 650 °C resulted in a higher surface area and reduced porosity of the HT, where the surface area of the HT increased from 79.595 m²/g to 115.558 m²/g, and the porosity decreased from 0.263 cm³/g to 0.198 cm³/g, similar to the findings by Helwani et al. (2013) and Pinthong et al. (2019). Table 2 also shows that extending the exposure at a calcination temperature of 750 °C or higher during the HT synthesis produced different results. The surface area of HT-CS 650 to HT-CS 750 decreased by 58.721 m²/g, while those for HT-CS 750 to HT-CS 850 were smaller by 28.517 m²/g.

The reduced surface area and porosity of the synthesized catalyst was due to the overheating of the HT at a calcination temperature of 750 °C and higher, which had a detrimental effect on the HT structure, including the surface area (Anuar & Abdullah, 2016). The high calcination temperature also affected the additional formation of the Mg-O periclase-like structure, as shown in the XRD spectra in Figure 4.

TGA ANALYSIS OF THE AS-SYNTHESIS CATALYST

The thermogravimetric analysis revealed the thermal decomposition of the freshly prepared dried HT samples at temperatures ranging from 30°C - 800°C. The TGA profiles of the HT samples in Figure 5 show that all samples exhibit significant weight loss. The as-synthesized (dried) HT-SS sample lost 38.84% of its total weight, while the HT-CS sample lost 79.67%. The profiles show three major stages of decomposition. The first stage of decomposition occurred between 37°C-250°C with the removal of the physically absorbed H₂O molecules (Dixit et al. 2013; Ramos-Ramirez et al. 2018). The saccharose-fueled HT showed the least weight loss of 12.89% in this stage. The ground coconut shell-fueled HT showed the highest weight loss of 52.54%. The ground coconut shell contains several organic compounds, including phenols, carbonyls, furans and alcohols, with boiling points below 200 °C (Hadanu & Apituley, 2016). In addition, the decomposition of hemicellulose occurred rapidly between 220 °C and 315 °C in HT-CS (Chen et al. 2019; Liyanage & Pieris, 2015). At the same time, saccharose decomposition occurred at 200 °C (Zhao et al. 2019). Hemicellulose contains various saccharide groups, such as galactose, glucose, rhamnose and arabinose (Yang et al. 2009), while saccharose only has two saccharide groups, glucose and fructose. The lignin decomposition began between 160 °C and 900°C; its slow decomposition was due to the rigid structure full of aromatic rings with branches (Yang et al. 2007). HT-CS lost 18.31% more weight than HT-SS. In the second stage of decomposition (251 °C–500 °C), the hydroxyl groups and interlayer carbonate ions, such as the CO₃²⁻ and OH⁻ ions, began to decompose (Dixit et al. 2013; Reyero et al. 2013). HT-CS lost 14.57% of its weight, while HT-SS lost 12.7%. HT-CS lost slightly more weight because the decomposition of the cellulose compound occurred between 315 °C and 400 °C at the same time as the lignin decomposition (Chen et al. 2019). The saccharose continues decomposing to a temperature of 400 °C (Zhao et al. 2019). The final stage of the thermal decomposition began at 500 °C, where the structure of layered hydroxide collapsed in the LDH framework (Anuar & Abdullah, 2016; Ramos-Ramirez et al. 2018; Reyero et al. 2013). The collapse of the LDH structure was verified by the XRD pattern of HT-CS 550, HT-CS 650, HT-CS 750, and HT-CS 850, as shown in Figure 4, and resulted in the formation of MgO and Al₂O₃ (Rezvani et al. 2015). The disappearance of peak in diffraction 11.7° as shown in Figure 4 proved the collapse of the layered structure.

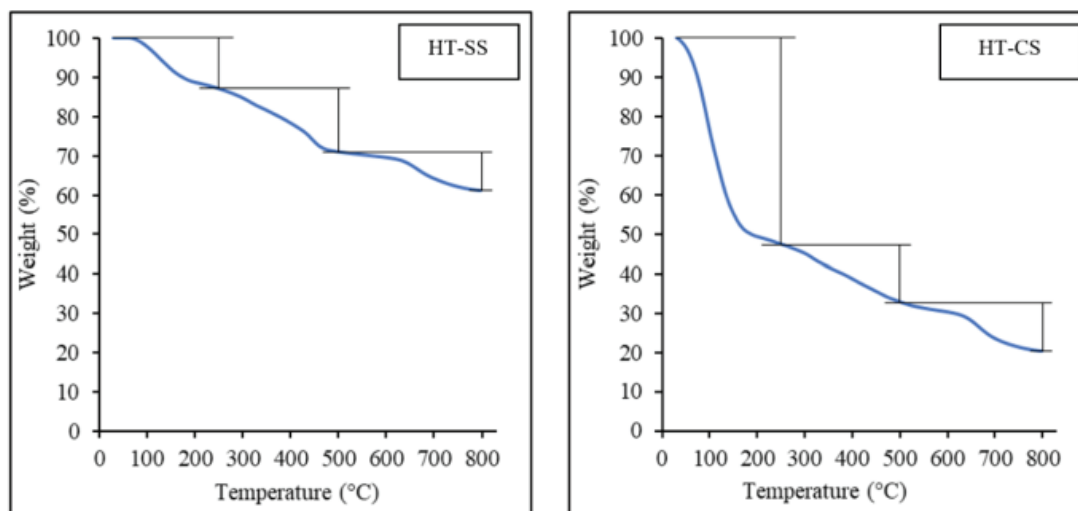


FIGURE 5. TGA profiles of the Hydrotalcite catalysts

FTIR ANALYSIS OF THE HYDROTALCITE CATALYST

The infrared spectra for HT-CS 650 and HT-SS 650 in Figure 6 show similar peak patterns even though the peak intensity differs slightly. The spectrum for HT is identical to those in previous studies (Coelho et al. 2017; Dixit et al. 2013; Martunus et al. 2011; Rezvani et al. 2015). The broad band at 3450-3500 cm^{-1} indicates the presence of a hydroxyl group in the interlayer of the brucite-like layers in the synthesized HT (Anuar & Abdullah, 2016; Dixit et al. 2013; Martunus et al. 2011). The 1634-1643 cm^{-1} band confirms the presence of H_2O in the interlayer structure of the HT samples (Dixit et al. 2013). The strong peak at 1375-1400 cm^{-1} represents the carbonate band on the interlayer gallery and serves as a bridge between cations, thus forming the layered structure of the synthesized HTs. The weak 1042-1092 cm^{-1} and 810-825 cm^{-1} bands confirm the existence of the covalent carbonate bond due to the

high calcination temperature (Anuar & Abdullah, 2016; Martunus et al. 2011). Some of the LDH structures of the samples collapsed with increasing temperature and trapped the CO_3^{2-} in the brucite-like structure (Anuar & Abdullah, 2016). The band at 575-630 cm^{-1} responds to the vibration of the metal oxides, Mg-O and Al-O (Martunus et al. 2011). The fuels used to synthesize the HT did not significantly affect the structure and bonding characteristics of the LDH. These findings are congruent with those of previous researchers (Anuar & Abdullah, 2016; Coelho et al. 2017; Ramimoghadam et al. 2015) who did not observe a significant peak after the LDH synthesis since all fuels were combusted and degraded at temperatures above 500 $^{\circ}\text{C}$. However, the fuel altered the porosity of the HT, as shown by the BET analysis. Therefore, it is possible to conclude that the presence of peaks 3450-3500 cm^{-1} , 1634-1643 cm^{-1} , 1375-1400 cm^{-1} , 1042-1092 cm^{-1} , 810-825 cm^{-1} and 575-630 cm^{-1} verifies the successful synthesis of HT catalyst for HT-CS 650 and HT-SS 650.

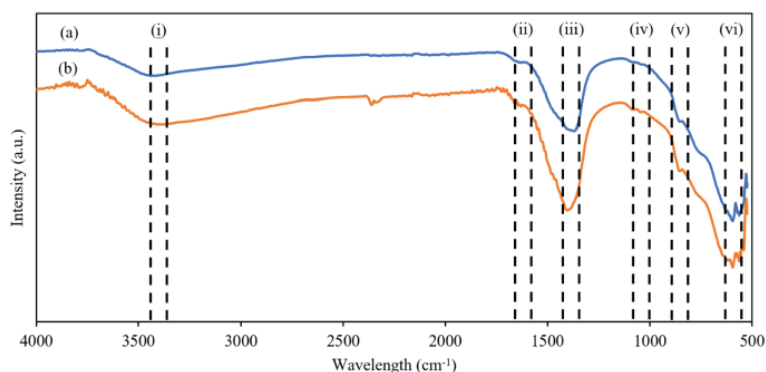


FIGURE 6. FTIR spectra of (a) HT-SS 650, (b) HT-CS 650, (i) 3450-3500 cm^{-1} , (ii) 1634-1643 cm^{-1} , (iii) 1375-1400 cm^{-1} , (iv) 1042-1092 cm^{-1} , (v) 810-825 cm^{-1} , and (vi) 575-630 cm^{-1}

CATALYTIC ACTIVITY OF THE SYNTHESIZED HYDROTALCITE

EFFECTS OF THE FUEL TYPE

This study began by synthesizing HT using saccharose and coconut shells as fuels. The fuels have different calorific values that are critical in enhancing the development of LDH structure during calcination (Anuar & Abdullah, 2016; Coelho et al. 2017). The similar FTIR spectra are due to the fuels having identical functional groups. However, there is a significant difference between the synthesized HTs regarding the performance of the catalytic activity of transesterification. Figure 7 shows the yield of

the FAME from the HT synthesized using different fuels. The ground coconut shell templated HT has the highest FAME yield of 93.25 %, while the HT with saccharose template yielded 74.14 % of FAME. The result of the HT produced using saccharose is similar to those obtained by Anuar & Abdullah (2016), namely 70.67 % with five hours of stirring. In the present study, changing the fuel when synthesizing the catalysts increased the biodiesel yield significantly by 19.11 %. The higher FAME yield of HT-CS 650 was due to its higher surface area of 115.558 m²/g compared to HT-SS 650, which has a surface area of 28.326 m²/g. The higher surface area of HT-CS 650 provided more active sites for the reaction. In summary, the HT yield depends on the types of organic fuel used.

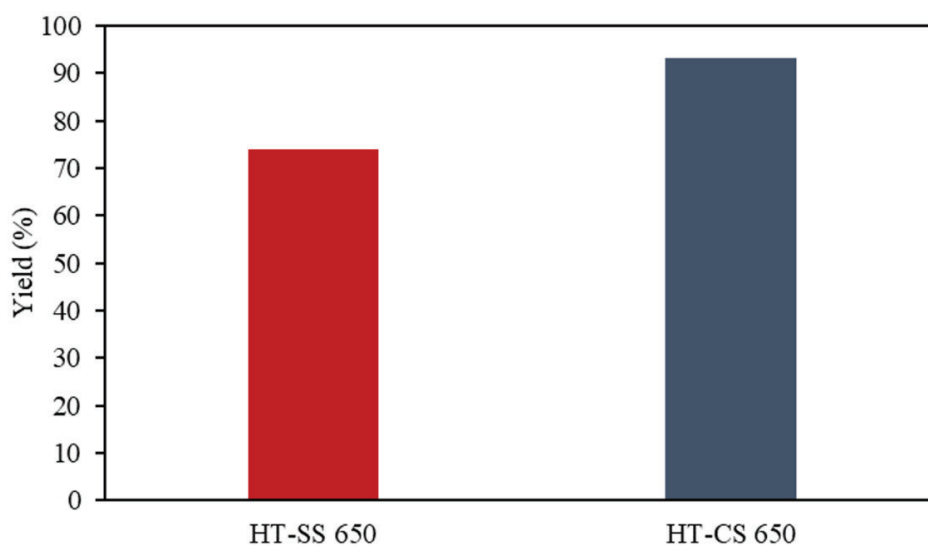


FIGURE 7. Catalytic activity with different types of fuel

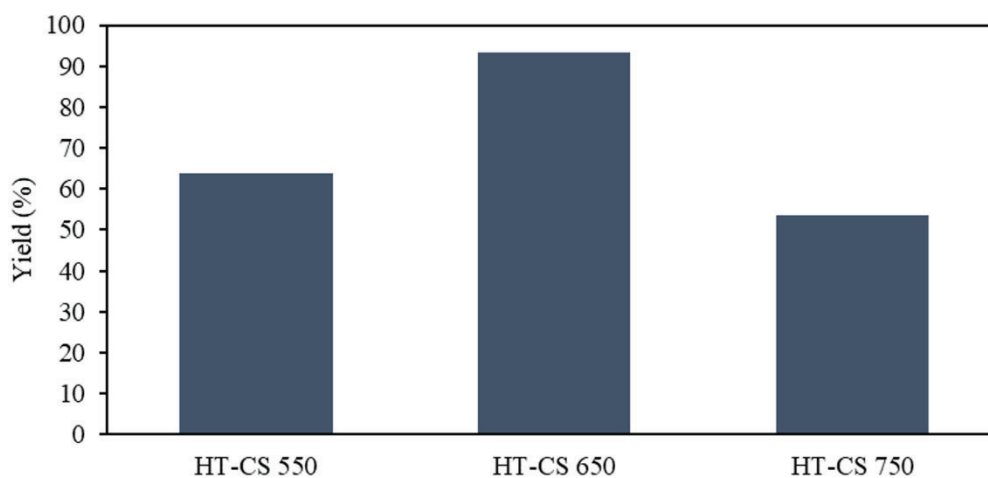


FIGURE 8. Catalytic activity at different calcination temperatures.

EFFECTS OF CALCINATION TEMPERATURE

This study determined whether calcination temperature affects the catalytic activity of the HT by performing transesterification of WCO using HT calcined at different temperatures. Previous studies have shown that the optimum calcination temperature for HT catalysts ranged between 500 °C-800 °C (Anuar & Abdullah, 2016; Dávila et al. 2008; Helwani et al. 2011; Martunus et al. 2011; Reyero et al. 2013). The calcination temperatures in this study were 550 °C, 650 °C and 750 °C. In the transesterification reaction with methanol, the WCO produced FAME made up of methyl myristate, methyl palmitate, methyl stearate, methyl oleate and methyl linoleate. Figure 8 shows the catalytic activity of the HT with varying calcination temperatures. The HT-CS calcined at 650 °C yielded the most FAME in a catalytic reaction with a five-hour reaction time, followed by the HTs calcined at 550 °C and 750 °C. The catalyst calcined at 650 °C produced the most FAME in the transesterification reaction. This result concurs with the findings of Anuar & Abdullah (2016) that the highest calcination temperature resulted in the formation of a divalent metal oxide, Mg-O, on the catalyst surface. However, at 750 °C, the yield of FAME decreased markedly to 53.60 % since the structure collapsed and reduced the surface area significantly, thus reducing the catalytic activity. The yield of FAME was similar to the trend of the BET surface area. Table 2 shows that increasing the calcination temperature from 550 °C to 650 °C resulted in a higher FAME yield that is directly proportional to the increase in the surface area of the BET. HT-CS 550 has a surface area of 79.595 m²/g and a 63.95 % yield of FAME. Increasing the calcination temperature to 650 °C increased the surface area by 35.963 m²/g and a 93.25 % yield of FAME. The larger surface area of the catalyst provided more active sites for the reaction, thus

increasing the yield of FAME. Calcination temperatures of 750 °C and higher caused the HT to overheat and had detrimental effects on the HT structure, including reduced surface area (Anuar et al. 2013), thus adversely affecting the performance of HT as a catalyst in transesterification reaction, as shown in Figure 8.

REUSABILITY OF THE CATALYST

In determining the reusability of the catalyst, this study performed three experimental runs of transesterification reaction with HT-CS 650 catalyst after using the fresh batch. Figure 9 shows the activity of HT-CS 650 for each cycle. The experimental run showed that the FAME yield of the best active HT catalyst decreased slightly in the third cycle. The fresh HT-CS 650 yielded 93.25% of FAME. However, its performance decreased by 7.5% in the several cycles of transesterification reaction with a consistent FAME yield. The reduced FAME yield was due to a minor structure collapse in the catalyst due to repeated calcination (Anuar & Abdullah, 2016), causing the carbonate content in the catalyst to diminish during the repeated re-calcination. The unique property, known as the memory effect, restored the catalytic activity during re-calcination and thus retained the FAME yield throughout the repeated transesterification reaction cycles (Anuar & Abdullah, 2016; Helwani et al. 2013). The experimental run proved that it is possible to use the HT in at least three cycles with a minimum FAME reduction of only 7.5 %. Even though the HT showed a good reusability potential, the amount of recovered catalyst decreased with each cycle. This study succeeded in recovering 50% of the total weight of the catalyst from the prior transesterification reaction. However, it could not conduct further experimental runs due to the small amount of HT investigated in this study.

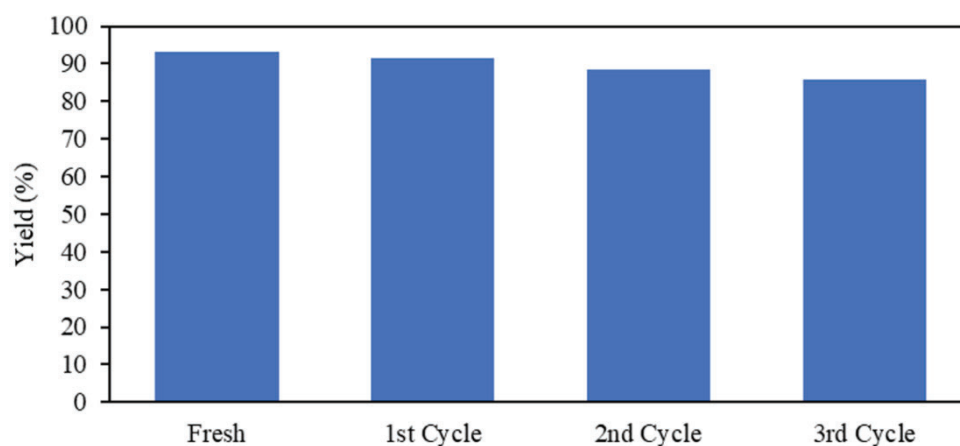


FIGURE 9. The catalytic activity of HT-CS 650 under a five-hour reaction time, 15:1 methanol to oil molar ratio, 8 % catalyst loading at 65 °C for three consecutive cycles.

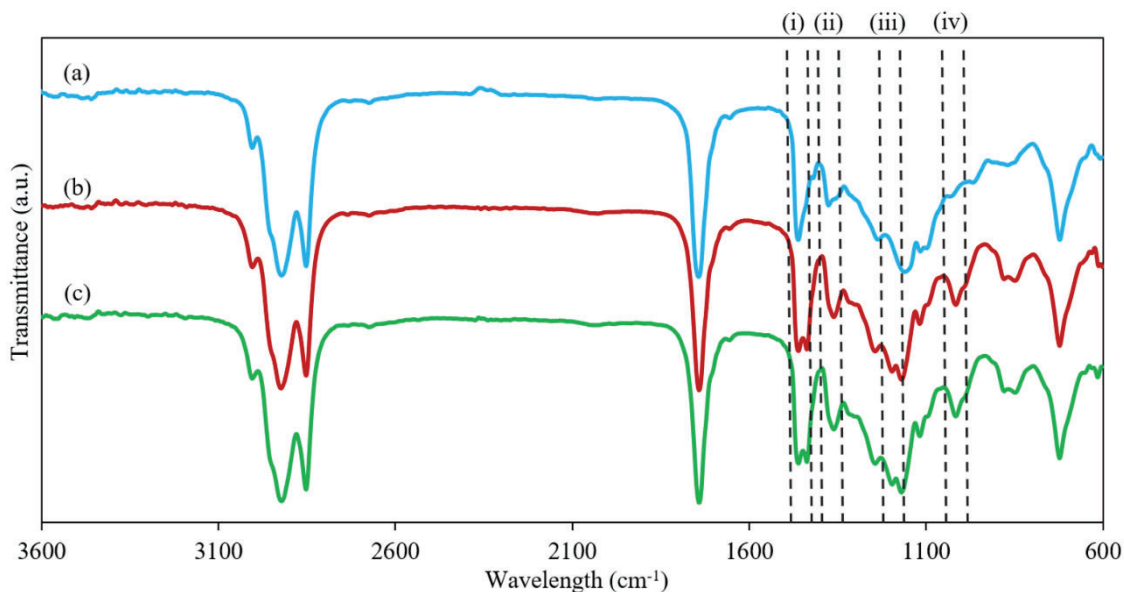


FIGURE 10. FTIR Spectra of (a) WCO, (b) Biodiesel produced using HT-SS 650, (c) Biodiesel produced from HT-CS 650, (i) 1412-1474 cm^{-1} , (ii) 1342-1386 cm^{-1} , (iii) 1152-1220 cm^{-1} , and (iv) 1002-1038 cm^{-1}

CHARACTERIZATION OF THE BIODIESEL

THE REACTION BETWEEN THE WCO AND METHANOL IN THE

reactor was for five hours and at 65 °C. The catalytic transesterification reaction of the oil with methanol produced FAME and glycerol as a byproduct. The FAME from the transesterification reaction was identified via the FTIR spectra. If the feedstock (WCO) and product, biodiesel (FAME), have the same vibration peaks, it is strong proof that there was no reaction between the reactants. The FTIR spectra of WCO and the biodiesels synthesized using HT as a catalyst in Figure 10 show several significant peaks, which help differentiate the WCO from the biodiesel. The most noticeable peaks appeared at 1196 cm^{-1} represents the methyl ester (CO)-C-CH₃ component in the FAME (Reyero et al. 2013). The formation of ethyl ester at 1435 cm^{-1} is the most significant since it is still classified as FAME (Marwan et al. 2015). The peak at 1377 cm^{-1} is the triglyceride compound vibration in the WCO spectra. However, this peak disappeared in both biodiesel spectra, indicating the successful conversion of the triglyceride into FAME after the transesterification reaction, similar to the findings by Rabelo et al. (2015). The peak at 1002-1038 cm^{-1} is attributed to C-O vibration, which concurs with the finding by Nisar et al. (2017), indicating the successful conversion of triglyceride into biodiesel. Therefore, it is possible to

conclude that the absence of peak 1377 cm^{-1} and the presence of peaks 1196 cm^{-1} , 1436 cm^{-1} and 1014 cm^{-1} confirms the successful catalytic reaction and complete conversion of the WCO into palm oil FAME.

CONCLUSION

This study has demonstrated that the coconut shell templated HT was more effective than the saccharose templated HT in the transesterification reaction at 65°C. Compared to the reference fuel, the coconut shells provided 446.665 more calories during combustion in the synthesis of the HT catalyst. The HT-CS catalyst calcined at 650 °C yielded the highest amount of biodiesel compared to calcination at 550 °C and 750 °C. HT-CS 650 yielded the highest amount of biodiesel (93.40 %) at 650 °C, while the reference catalyst using saccharose as fuel yielded 76.01 %. Treatment at an excessive temperature of 750 °C caused the layered structure to collapse and initiate the formation of an impurity phase, which resulted in a low biodiesel yield. In addition, the test on the robustness of the HT-CS 650 catalyst showed that it is possible to reuse the catalyst for up to three cycles with a minimum reduction of FAME yield of only 7.5 %. The advantages of this catalyst are easy separation of the catalyst, possible recycling and encourage the use of waste materials, including coconut shells, as fuel in the synthesis of HT catalysts.

ACKNOWLEDGEMENTS

The authors are grateful to the Fundamental Research Grant Scheme (FGRS/1/2023/TK08/ UKM/03/3), Long-Term Research Grant Scheme (LGRS/MRUN/F2/01/2019), Excellent Graduate Assistantship (55360117005), Yayasan Tengku Abdullah Scholarship (55360117005), and Short-Term Research Grant (STR17077) for funding this research.

DECLARATION OF COMPETING INTEREST

None.

REFERENCES

- Ajien, A., Idris, J., Md Sofwan, N., Husen, R. & Seli, H., 2023. Coconut shell and husk biochar: A review of production and activation technology, economic, financial aspect and application. *Waste Management & Research* 41(1): pp.37-51. DOI: <https://doi.org/10.1177/0734242X221127167>.
- Al-Oqla, F.M., Faris, H., Habib, M. & Castillo, P.A., 2023. Evolving genetic programming tree models for predicting the mechanical properties of green fibers. *Emerging Science Journal* 7(6): 1863-1874. DOI: <https://doi.org/10.28991/ESJ-2023-07-06-02>.
- Anuar, M.R., Abdullah, A.Z. & Othman, M.R., 2013. Etherification of glycerol to polyglycerols over hydrotalcite catalyst prepared using a combustion method. *Catalysis Communications* 32: 67-70. DOI: <https://doi.org/10.1016/j.catcom.2012.12.007>.
- Anuar, M. R., & Abdullah, A. Z. 2016. Ultrasound-assisted biodiesel production from waste cooking oil using hydrotalcite prepared by combustion method as catalyst. *Applied Catalysis A: General* 514: 214-223. DOI: <https://doi.org/10.1016/j.apcata.2016.01.023>.
- Atadashi, I. M., Aroua, M. K., Aziz, A. A., & Sulaiman, N. M. N. 2012. The effects of water on biodiesel production and refining technologies: A review. *Renewable and Sustainable Energy Reviews* 16(5): 3456-3470. DOI: <https://doi.org/10.1016/j.rser.2012.03.004>.
- Bello, S.A., Agunsoye, J.O., Adebisi, J.A., Kolawole, F.O. & Hassan, S.B., 2016. Physical properties of coconut shell nanoparticles. *Kathmandu University Journal of Science, Engineering and Technology* 12(1): 63-79. DOI: <https://ir.unilag.edu.ng/handle/123456789/8570>.
- Borges, M. E., & Diaz, L. 2012. *Recent developments on heterogeneous catalysts for biodiesel production by oil esterification and transesterification reactions: A review. Renewable and Sustainable Energy Reviews* 16(5): 2839-2849. DOI: <https://doi.org/10.1016/j.rser.2012.01.071>.
- Bhojaraj, Harley, P., & Rajamathi, M. 2019. Cannizzaro reactions over calcined hydrotalcite. *Applied Clay Science* 174: 86-89. DOI: <https://doi.org/10.1016/j.clay.2019.03.028>.
- Che Hamzah, N. H., Khairuddin, N., Siddique, B. M. & Hassan, M. A. 2020. Potential of *Jatropha curcas* L. as biodiesel feedstock in Malaysia: A concise review. *Processes* 8(7): 786. DOI: <https://doi.org/10.3390/pr8070786>.
- Chen, W.H., Wang, C.W., Ong, H.C., Show, P.L. & Hsieh, T.H., 2019. Torrefaction, pyrolysis and two-stage thermodegradation of hemicellulose, cellulose and lignin. *Fuel* 258: 116168. DOI: <https://doi.org/10.1016/j.fuel.2019.116168>.
- Ciobanu, A., Ruellan, S., Mallard, I., Landy, D., Gennequin, C., Siffert, S., & Fourmentin, S. 2013. Cyclodextrin-intercalated layered double hydroxides for fragrance release. *Journal of Inclusion Phenomena and Macrocyclic Chemistry* 75: 333-339. DOI: <https://doi.org/10.1007/s10847-012-0227-4>.
- Coelho, A., Perrone, O. M., Gomes, E., Da-Silva, R., Thoméo, J. C., & Boscolo, M. 2017. Mixed metal oxides from sucrose and cornstarch templated hydrotalcite-like LDHs as catalysts for ethyl biodiesel synthesis. *Applied Catalysis A: General* 532: 32-39. DOI: <https://doi.org/10.1016/j.apcata.2016.12.012>.
- Daud, W.M.A.W. & Ali, W.S.W., 2004. Comparison on pore development of activated carbon produced from palm shell and coconut shell. *Bioresource Technology* 93(1): 63-69. DOI: <https://doi.org/10.1016/j.biortech.2003.09.015>.
- Dávila, V., Lima, E., Bulbulian, S., & Bosch, P. 2008. Mixed Mg (Al) O oxides synthesized by the combustion method and their recrystallization to hydrotalcites. *Microporous and Mesoporous Materials* 107(3): 240-246. DOI: <https://doi.org/10.1016/j.micromeso.2007.03.013>.
- Dixit, M., Mishra, M., Joshi, P.A. & Shah, D.O., 2013. Physico-chemical and catalytic properties of Mg–Al hydrotalcite and Mg–Al mixed oxide supported copper catalysts. *Journal of Industrial and Engineering Chemistry* 19(2): 458-468. DOI: <https://doi.org/10.1016/j.jiec.2012.08.028>.
- Dudley, B. 2019. BP statistical review of world energy 2018. *British Petroleum Statistical Review of World Energy*, Bplc. editor; Pureprint Group Limited, UK. <http://www.bp.com/statisticalreview> [11 February 2019].
- FAO. 2017. Malaysian Production of Coconut. <http://www.fao.org/faostat/en/#data/QC>. [20 November 2018].
- Fraile, J.M., García, N., Mayoral, J.A., Pires, E. & Roldán, L., 2009. The influence of alkaline metals on

- the strong basicity of Mg–Al mixed oxides: the case of transesterification reactions. *Applied Catalysis A: General* 364 (1-2): 87-94. DOI: <https://doi.org/10.1016/j.apcata.2009.05.031>.
- Gao, L., & Goldfarb, J. L. 2019. Solid waste to biofuels and heterogeneous sorbents via pyrolysis of wheat straw in the presence of fly ash as an in-situ catalyst. *Journal of Analytical and Applied Pyrolysis* (137): 96-105. DOI: <https://doi.org/10.1016/j.jaap.2018.11.014>.
- Hadanu, R. & Apituley, D.A.N. 2016. Volatile Compounds Detected in Coconut Shell Liquid Smoke through Pyrolysis at a Fractioning Temperature of 350-420° C. *Makara Journal of Science*: 95-100. DOI: <https://doi.org/10.7454/mss.v20i3.6239>.
- Hall, S. R., Bolger, H., & Mann, S. 2003. Morphosynthesis of complex inorganic forms using pollen grain templates. *Chemical Communications* 22: 2784-2785. DOI: <https://doi.org/10.1039/B309877J>.
- Helwani, Z., Aziz, N., Bakar, M. Z. A., Mukhtar, H., Kim, J., & Othman, M. R. 2013. Conversion of *Jatropha curcas* oil into biodiesel using re-crystallized hydrotalcite. *Energy Conversion and Management* 73: 128-134. DOI: <https://doi.org/10.1016/j.enconman.2013.04.004>.
- Herring, T.C. & Thuo, J.N., 2022. Engineering and durability properties of modified coconut shell concrete. DOI: <https://doi.org/10.28991/CEJ-2022-08-02-013>.
- Higai, D., Huang, Z. & Qian, E.W., 2021. Preparation and surface characteristics of phosphoric acid-activated carbon from coconut shell in air. *Environmental Progress & Sustainable Energy* 40(2): p.e13509. DOI: <https://doi.org/10.1002/ep.13509>.
- Huaping, Z. H. U., Zongbin, W. U., Yuanxiong, C., Zhang, P., Shijie, D. U. A. N., Xiaohua, L. I. U., & Zongqiang, M. A. O. 2006. Preparation of biodiesel catalyzed by solid super base of calcium oxide and its refining process. *Chinese Journal of Catalysis* 27 (5): 391-396. DOI: [https://doi.org/10.1016/S1872-2067\(06\)60024-7](https://doi.org/10.1016/S1872-2067(06)60024-7).
- Ismail, A. & Isa, N.M., 2017. Potential of Coconut Shell Replacement as Coarse Aggregate in Hot Mix Asphalt. *Jurnal Kejuruteraan* 29(1): pp.77-81.
- Ka, H., Sa, K. & Yang, T. 2013. The management of waste cooking oil: a preliminary survey. *Health and Environ J* 4: 76-81.
- Kabir, I., Yacob, M., & Radam, A., 2014. Households' awareness, attitudes and practices regarding waste cooking oil recycling in Petaling, Malaysia. *IOSR Journal of Environmental Science, Toxicology and Food Technology* 8(10): 45-51.
- Kim, D., Lee, K. & Park, K.Y., 2016. Upgrading the characteristics of biochar from cellulose, lignin, and xylan for solid biofuel production from biomass by hydrothermal carbonization. *Journal of industrial and Engineering Chemistry* 42: 95-100. DOI: <https://doi.org/10.1016/j.jiec.2016.07.037>.
- Lazarova, T., Kovacheva, D., Georgieva, M., Tzankov, D., Tyuliev, G., Spassova, I. & Naydenov, A. 2019. Tunable nanosized spinel manganese ferrites synthesized by solution combustion method. *Applied Surface Science* 496: 143571. DOI: <https://doi.org/10.1016/j.apsusc.2019.143571>.
- Lee, C. H., Kim, S., Yoon, H. J., Yoon, C. W., & Lee, K. B. 2021. Water gas shift and sorption-enhanced water gas shift reactions using hydrothermally synthesized novel Cu–Mg–Al hydrotalcite-based catalysts for hydrogen production. *Renewable and Sustainable Energy Reviews* 145: 111064. DOI: <https://doi.org/10.1016/j.rser.2021.111064>.
- Li, W., Yang, K., Peng, J., Zhang, L., Guo, S. & Xia, H., 2008. Effects of carbonization temperatures on characteristics of porosity in coconut shell chars and activated carbons derived from carbonized coconut shell chars. *Industrial Crops and Products* 28 (2): 190-198. DOI: <https://doi.org/10.1016/j.indc.2008.02.012>.
- Liyanage, C.D. & Pieris, M., 2015. A physico-chemical analysis of coconut shell powder. *Procedia Chemistry* 16: 222-228. DOI: <https://doi.org/10.1016/j.proche.2015.12.045>.
- Martunus, Othman, M.R. & Fernando, W.J.N., 2011. Elevated temperature carbon dioxide capture via reinforced metal hydrotalcite. *Microporous and Mesoporous Materials* 138(1-3): 110-117. DOI: <https://doi.org/10.1016/j.micromeso.2010.09.023>.
- Marwan, Suhendrayatna & Indarti, E. 2015. Preparation of biodiesel from microalgae and palm oil by direct transesterification in a batch microwave reactor. In *Journal of Physics: Conference Series* vol. 622, no. 1, p. 012040. IOP Publishing. DOI: <https://doi.org/10.1088/1742-6596/622/1/012040>.
- Nayab, R., Imran, M., Ramzan, M., Tariq, M., Taj, M. B., Akhtar, M. N., & Iqbal, H. M. 2022. Sustainable biodiesel production via catalytic and non-catalytic transesterification of feedstock materials – A review. *Fuel* 328: 125254. DOI: <https://doi.org/10.1016/j.fuel.2022.125254>.
- Naylor, R. L., & Higgins, M. M. 2018. The rise in global biodiesel production: Implications for food security. *Global Food Security* 16: 75-84. DOI: <https://doi.org/10.1016/j.gfs.2017.10.004>.
- Nisar, J., Razaq, R., Farooq, M., Iqbal, M., Khan, R.A., Sayed, M., Shah, A. & ur Rahman, I. 2017. Enhanced biodiesel production from *Jatropha* oil using calcined waste animal bones as catalyst. *Renewable Energy* 101: 111-119. DOI: <https://doi.org/10.1016/j.renene.2016.08.048>.
- Pinthong, P., Praserttham, P. & Jongsomjit, B. 2019. Effect of calcination temperature on Mg–Al layered double hydroxides (LDH) as promising

- catalysts in oxidative dehydrogenation of ethanol to acetaldehyde. *Journal of Oleo Science* 68(1): 95-102. DOI: <https://doi.org/10.5650/jos.ess18177>.
- Rabelo, S.N., Ferraz, V.P., Oliveira, L.S. & Franca, A.S. 2015. FTIR analysis for quantification of fatty acid methyl esters in biodiesel produced by microwave - assisted transesterification. *International Journal of Environmental Science and Development* 6 (12): 964. DOI: <https://doi.org/10.7763/IJES D.2015.V6.730>.
- Rahul, R., Satyarthi, J. K. & Srinivas. D. 2011. Lanthanum and zinc incorporated hydrotalcites as solid base catalysts for biodiesel and biolubricants production.
- Ramimoghadam, D., Bagheri, S., & Abd Hamid, S. B. 2015. Stable monodisperse nanomagnetic colloidal suspensions: an overview. *Colloids and Surfaces B: Biointerfaces* 133: 388-411. DOI: <https://doi.org/10.1016/j.colsurfb.2015.02.003>.
- Ramos-Ramirez, E., Gutiérrez-Ortega, N., Tzompantzi, F., Gomez, C. M., del Angel, G., Herrera-Pérez, G., Serafin-Muñoz, A.H., & Tzompantzi-Flores, C. 2018. Activated hydrotalcites obtained by coprecipitation as photocatalysts for the degradation of 2, 4, 6-trichlorophenol. *Advances in Materials Science and Engineering*: 1-15. DOI: <https://doi.org/10.1155/2018/8267631>.
- Reyero, I., Velasco, I., Sanz, O., Montes, M., Arzamendi, G. & Gandía, L.M., 2013. Structured catalysts based on Mg–Al hydrotalcite for the synthesis of biodiesel. *Catalysis Today* 216: 211-219. DOI: <https://doi.org/10.1016/j.cattod.2013.04.022>.
- Rezvani, Z., Rad, F.A. & Khodam, F. 2015. Synthesis and characterization of Mg–Al-layered double hydroxides intercalated with cubane-1, 4-dicarboxylate anions. *Dalton Transactions* 44(3): 988-996. DOI: <https://doi.org/10.1039/C4DT03152K>.
- Salmah, H., Koay, S.C. & Hakimah, O. 2013. Surface modification of coconut shell powder filled polylactic acid biocomposites. *Journal of Thermoplastic Composite Materials* 26(6): 809-819. DOI: <https://doi.org/10.1177/0892705711429981>.
- Selvam, N.C.S., Kumar, R.T., Kennedy, L.J. & Vijaya, J.J., 2011. Comparative study of microwave and conventional methods for the preparation and optical properties of novel MgO-micro and nano-structures. *Journal of Alloys and Compounds* 509(41): 9809-9815. DOI: <https://doi.org/10.1016/j.jallcom.2011.08.032>.
- Shekoochi, K., Hosseini, F.S., Haghghi, A.H. & Sahrayian, A. 2017. Synthesis of some Mg/Co-Al type nano hydrotalcites and characterization. *MethodsX* 4: 86-94. DOI: <https://doi.org/10.1016/j.mex.2017.01.003>.
- Sobhana, S. L., Bogati, D. R., Reza, M., Gustafsson, J., & Fardim, P. 2016. Cellulose biotemplates for layered double hydroxides networks. *Microporous and Mesoporous Materials* 225: 66-73. DOI: <https://doi.org/10.1016/j.micromeso.2015.12.009>.
- Suriyanarayanan, N., Nithin, K.K. & Bernardo, E., 2009. Mullite glass ceramics production from coal ash and alumina by high temperature plasma. *Journal of Non-Oxide Glasses* 1(4): 247-260.
- Yabushita, M., Shibayama, N., Nakajima, K., & Fukuoka, A. 2019. Selective glucose-to-fructose isomerization in ethanol catalyzed by hydrotalcites. *ACS Catalysis* 9(3): 2101-2109. DOI: <https://doi.org/10.1021/acscatal.8b05145>.
- Yang, H., Yan, R., Chen, H., Lee, D.H. & Zheng, C., 2007. Characteristics of hemicellulose, cellulose and lignin pyrolysis. *Fuel* 86(12-13): 1781-1788. DOI: <https://doi.org/10.1016/j.fuel.2006.12.013>.
- Zervos, A., 2018. REN21, Renewables 2018 Global Status Report. <http://www.ren21.net/gsr-2018/> [12 February 2019].
- Ziegler, J. 2013. Burning food crops to produce biofuels is a crime against humanity. *The Guardian* 26. <https://www.theguardian.com/global-development/povertymatters/2013/nov/26/burning-food-crops-biofuels-crime-humanity> [10 November 2018].
- Zhao, Z., Sakai, S., Wu, D., Chen, Z., Zhu, N., Huang, C., Sun, S., Zhang, M., Umemura, K. & Yong, Q., 2019. Further exploration of sucrose–citric acid adhesive: Investigation of optimal hot-pressing conditions for plywood and curing behavior. *Polymers* 11(12): 1996. DOI: <https://doi.org/10.3390/polym11121996>.